



Occurrence of *Pestalotiopsis lushanensis* causing leaf blight on Buddhist pine in China

Xiang-rong Zheng · Mao-jiao Zhang ·
Feng-mao Chen

Accepted: 22 November 2021 / Published online: 10 January 2022
© Koninklijke Nederlandse Planteziektenkundige Vereniging 2022

Abstract Buddhist pine (*Podocarpus macrophyllus*) is a widely cultivated evergreen tree species with high ornamental and economic value. Recently, severe leaf blight on Buddhist pine was detected in Anhui Province, China. Seven single-spore isolates obtained from symptomatic samples were identified as *Pestalotiopsis lushanensis* on the basis of morphology and multilocus (internal transcribed spacer region, translation elongation factor 1- α and β -tubulin) phylogenetic analysis. Pathogenicity tests of potted Buddhist pine seedlings revealed that regardless of whether a conidial suspension or mycelial disk was used, inoculation of *P. lushanensis* could result in leaf blight symptoms similar to those observed in the field. These results have important implications for further research on targeted prevention and control strategies.

Keywords Buddhist pine · Leaf blight ·
Pestalotiopsis lushanensis

Buddhist pine (*Podocarpus macrophyllus* [Thunb.] D. Don) is a long-lived tree species that is widely cultivated for landscaping in subtropical regions of China (Luo et al., 2020). In addition to its aesthetic

characteristics, Buddhist pine is also recognized for the pharmacological uses of its leaves (Wang et al., 2017). Owing to its ornamental and economic value, Buddhist pine has promising development prospects. However, in recent years, fungal diseases of Buddhist pine have become increasingly serious and restrictive to its cultivation and industrial development.

Pestalotiopsis-like genera form a species-rich fungal group with appendage-bearing conidia in family Sporocadaceae (Chen et al., 2018; Liu et al., 2019). *Pestalotiopsis* spp. were previously considered opportunistic or weak phytopathogens that could cause little damage to ornamental plants (Pirone, 1978). However, in recent years, abundant studies have confirmed that species of *Pestalotiopsis* are responsible for diseases such as grey blight, leaf blight, canker, dieback and various postharvest diseases, resulting in a substantial reduction in commercial production (Akin-sanmi et al., 2017; Chen et al., 2018; Liu et al., 2017; Maharachchikumbura et al., 2012; Silva et al., 2020).

The classification of *Pestalotiopsis* species was traditionally limited to a host-based taxonomic system and conidial characters (Hu et al., 2007; Jeewon et al., 2003). However, the morphological features excessively overlapped between species, which restricted research on this type of fungus. Maharachchikumbura et al. (2012) identified the internal transcribed spacer (ITS) region, translation elongation factor 1- α (TEF), and β -tubulin (TUB) genes as the best genetic markers for distinguishing taxa in this group; together with conidial morphology, these markers provide a precise

X. Zheng · M. Zhang · F. Chen (✉)
Collaborative Innovation Center of Sustainable Forestry
in Southern China, College of Forestry, Nanjing Forestry
University, Nanjing 210037, Jiangsu, China
e-mail: cfengmao@njfu.edu.cn

tool for distinguishing *Pestalotiopsis* fungi at the species level (Chen et al., 2018; Maharachchikumbura et al., 2014; Zhang et al., 2021).

In March 2019, during a disease investigation in Quanjiao County, Anhui Province, a severely harmful Podocarpus leaf blight was found, with an incidence rate of over 60%. The purpose of this study was to identify the pathogen causing Podocarpus leaf blight by combining morphological and molecular biological methods.

Buddhist pine leaves with typical symptoms were sampled at Nanping Mountain Forest Park in Quanjiao County (118°16'22"N, 32°5'7"E), Anhui Province, China. Leaf Sects. (4 cm²) were excised from lesion margins, surface sterilized as described by Zheng et al. (2020a), and placed onto potato dextrose agar (PDA) plates amended with 100 µg/ml ampicillin. The samples were then incubated at 25 °C in darkness. The hyphal tip from emerging mycelium was subsequently transferred to a new PDA plate, and pure culture was obtained by monosporic isolation.

Seven single-spore isolates were selected for morphological characterization.

Cultural and conidial characteristics were recorded seven days post inoculation (dpi). The morphological features of conidia were recorded according to the standard described by Maharachchikumbura et al. (2014). Fifty measurements per structure were taken under a ZEISS microscope (Carl Zeiss, Germany) at 100× magnification.

Total DNA of all isolates was extracted using the cetyltrimethylammonium bromide (CTAB) method according to Wang et al. (2020). DNA concentrations were quantified and manually adjusted to 100 ng/µl for polymerase chain reaction (PCR) using a NanoDrop 2000 spectrophotometer (Thermo Fisher Scientific, Madison, WI, USA). Primer pairs ITS1/ITS4 (White et al., 1990), T1 (O'Donnell & Cigelnik, 1997)/Bt-2b (Glass & Donaldson, 1995), and EF1-728F (Carbone & Kohn, 1999)/EF-2 (O'Donnell et al., 1998) were utilized to amplify the ITS region and portions of the TUB and TEF genes, respectively. The PCR assays were run in a volume of 50 µl as described by Zheng et al., (2020a, b). Amplifications were performed on an Eppendorf Nexus Thermal Cycler (Eppendorf) using the following amplification conditions: initial denaturation of 94 °C for 4 min, followed by 30 cycles of 94 °C for 30 s; 55 °C for ITS, 55 °C for TUB, and 52 °C for TEF for 30 s;

72 °C for 45 s; and a final extension step at 72 °C for 10 min. Amplicons were subjected to sequencing by Shanghai Jie Li Biological Technology Company (Shanghai, China), using both forward and reverse primers for each locus. All sequences obtained in this study were deposited into GenBank (Table 1).

Reference *Pestalotiopsis* spp. Sequences, including type specimens (ex-epitype or ex-holotype culture), were retrieved from GenBank following Liu et al. (2017), Maharachchikumbura et al. (2014) and Tsai et al. (2020), respectively. *Neopestalotiopsis saprophytica* (MFLUCC 12–0282) was included as the outgroup. Multiple sequence alignments were performed using BioEdit v. 7.0.5 (<http://www.mbio.ncsu.edu/bioedit/page2.html>) and then checked visually and improved manually to obtain the maximal aligned sets of sequences. Gaps were regarded as a fifth character, which had equal weight in the alignment.

The phylogenetic analysis for the concatenated dataset (ITS + TEF + TUB) were conducted under the maximum likelihood (ML) and Bayesian inference (BI) criteria, using MEGA 7 (Kumar et al., 2016) and MrBayes 3.2.6 (Ronquist et al., 2012), respectively. Maximum likelihood (ML) analyses were conducted using the general time-reversible model with nearest-neighbour interchange (NNI) method, and clade stability was determined from 1,000 bootstrap replicates (Kumar et al., 2016). MEGA v.7 was used to infer the best model of nucleotide substitution according to the corrected Akaike information criterion (AICc) for the ML analyses. For BI analysis, two analyses in parallel were performed with four Markov chains, evaluating 50 million generations, with samples taken every 1000th generation. Posterior probabilities (PP) were calculated after discarding the first 25% of generations as burn-in. Bootstrap values ≥ 70 and posterior probabilities ≥ 0.99 were taken as evidence for support of the branches (Huelsenbeck & Rannala, 2004).

The seven isolates used for morphological characterization were evaluated to determine their pathogenicity.

Two pathogenicity assays of each isolate were conducted using 1-year-old potted seedlings of Buddhist pine with either conidial suspensions or mycelial plugs. All isolates were cultured on PDA at 25 °C as mentioned above, and a spore suspension was obtained by rushing 30-day-old cultures with sterile distilled water and adjusting the concentration to 10⁵ conidia/ml with a haemocytometer.

Table 1 Descriptions and sequence accession numbers used in the phylogenetic study

Species	Culture accession number ^a	Host/Substrate	Location	GenBank accession number ^b		
				ITS	TUB	TEF
<i>Neopestalotiopsis saprophytica</i>	MFLUCC 12–0282*	<i>Magnolia</i> sp.	China	JX398982	JX399017	JX399048
<i>Pestalotiopsis adusta</i>	ICMP 6088*	On refrigerator door PVC gasket	Fiji	JX399006	JX399037	JX399070
<i>P. aggestorum</i>	LC6301*	<i>Camellia sinensis</i>	China	KX895015	KX895348	KX895234
<i>P. anacardiacearum</i>	IFRDCC 2397*	<i>Mangifera indica</i>	China	KC247154	KC247155	KC247156
<i>P. arceuthobii</i>	CBS 434.65*	<i>Arceuthobium campylopodum</i>	USA	KM199341	KM199427	KM199516
<i>P. arengae</i>	CBS 331.92*	<i>Arenga undulatifolia</i>	Singapore	KM199340	KM199426	KM199515
<i>P. australasiae</i>	CBS 114,126*	<i>Knightia</i> sp.	New Zealand	KM199297	KM199409	KM199499
<i>P. australis</i>	CBS 114,193*	<i>Grevillea</i> sp.	Australia	KM199332	KM199383	KM199475
<i>P. biciliata</i>	CBS 124,463*	<i>Platanus x hispanica</i>	Slovakia	KM199308	KM199399	KM199505
<i>P. brachiata</i>	LC2988*	<i>Camellia</i> sp.	China	KX894933	KX895265	KX895150
<i>P. brassicae</i>	CBS 170.26*	<i>Brassica napus</i>	New Zealand	KM199379	—	KM199558
<i>P. camelliae</i>	MFLUCC 12–0277*	<i>Camellia japonica</i>	China	JX399010	JX399041	JX399074
<i>P. chamaeropsis</i>	CBS 186.71*	<i>Chamaerops humilis</i>	Italy	KM199326	KM199391	KM199473
<i>P. chinensis</i>	MFLUCC 12–0273*	Dead plant material	China	JX398995	—	—
<i>P. clavata</i>	MFLUCC 12–0268*	<i>Buxus</i> sp.	China	JX398990	JX399025	JX399056
<i>P. colombiensis</i>	CBS 118,553*	<i>Eucalyptus euro-grandis</i>	Colombia	KM199307	KM199421	KM199488
<i>P. digitalis</i>	ICMP 5434*	<i>Digitalis purpurea</i>	New Zealand	KP781879	KP781883	—
<i>P. dilucida</i>	LC3232*	<i>Camellia sinensis</i>	China	KX894961	KX895293	KX895178
<i>P. diplocloisiae</i>	CBS 115,587*	<i>Diplocloisia glaucescens</i>	China	KM199320	KM199419	KM199486
<i>P. disseminata</i>	CBS 118,552	<i>Eucalyptus botryoides</i>	New Zealand	MH553986	MH554652	MH554410
<i>P. diversiseta</i>	MFLUCC 12–0287*	<i>Rhododendron</i> sp.	China	JX399009	JX399040	JX399073
<i>P. dracontomelon</i>	MFLUCC 10–0149*	<i>Dracontomelon dao</i>	Thailand	KP781877	—	KP781880
<i>P. ericacearum</i>	IFRDCC 2439*	<i>Rhododendron delavayi</i>	China	KC537807	KC537821	KC537814
<i>P. furcata</i>	MFLUCC 12–0054*	<i>Camellia sinensis</i>	Thailand	JQ683724	JQ683708	JQ683740
<i>P. gaultheria</i>	IFRD 411–014*	<i>Gaultheria forrestii</i>	China	KC537805	KC537819	KC537812
<i>P. gibbosa</i>	NOF 3175*	<i>Gaultheria shallon</i>	Canada	LC311589	LC311590	LC311591
<i>P. grandis-urophylla</i>	E-72–02	<i>Eucalyptus grandis</i>	Brazil	KU926708	KU926716	KU926712
	E-72–03	<i>Eucalyptus grandis</i>	Brazil	KU926709	KU926717	KU926713
<i>P. grevilleae</i>	CBS 114,127*	<i>Grevillea</i> sp.	Australia	KM199300	KM199407	KM199504
<i>P. hawaiiensis</i>	CBS 114,491*	<i>Leucospermum</i> sp. cv. 'Coral'	USA	KM199339	KM199428	KM199514
<i>P. hispanica</i>	CBS 115,391*	<i>Protea</i> sp.	Spain	MH553981	MH554640	MH554399
<i>P. hollandica</i>	CBS 265.33*	<i>Sciadopitys veitcillata</i>	Netherlands	KM199328	KM199388	KM199481
<i>P. humus</i>	CBS 336.97*	Soil	Papua New Guinea	KM199317	KM199420	KM199484
<i>P. inflexa</i>	MFLUCC 12–0270*	Unidentified tree	China	JX399008	JX399039	JX399072
<i>P. intermedia</i>	MFLUCC 12–0259*	Unidentified tree	China	JX398993	JX399028	JX399059
<i>P. jesteri</i>	CBS 109,350*	<i>Fragariae bodenii</i>	Papua New Guinea	KM199380	KM199468	KM199554

Table 1 (continued)

Species	Culture accession number ^a	Host/Substrate	Location	GenBank accession number ^b		
				ITS	TUB	TEF
<i>P. jiangxiensis</i>	LC4399*	<i>Camellia</i> sp.	China	KX895009	KX895341	KX895227
<i>P. jinchanghensis</i>	LC6636*	<i>Camellia sinensis</i>	China	KX895028	KX895361	KX895247
<i>P. kenyana</i>	CBS 442.67*	<i>Coffea</i> sp.	Kenya	KM199302	KM199395	KM199502
<i>P. knightiae</i>	CBS 114,138*	<i>Knightia</i> sp.	New Zealand	KM199310	KM199408	KM199497
<i>P. krabiensis</i>	MFLUCC 16–0260*	<i>Pandanus</i> sp.	Thailand	MH388360	MH412722	MH388395
<i>P. kunmingensis</i>	PSHI2002Endo766*	<i>Podocarpus macrophyllus</i>	China	AY373376	DQ333576	—
<i>P. leucadendri</i>	CBS 121,417*	<i>Leucadendron</i> sp.	South Africa	MH553987	MH554654	MH554412
<i>P. licualacola</i>	HGUP 4057*	<i>Licuala grandis</i>	China	KC492509	KC481683	KC481684
<i>P. linearis</i>	MFLUCC 12–0271*	<i>Trachelospermum</i> sp.	China	JX398992	JX399027	JX399058
<i>P. longiappendiculata</i>	LC3013*	<i>C. sinensis</i>	China	KX894939	KX895271	KX895156
<i>P. lushanensis</i>	LC4344*	<i>Camellia</i> sp.	China	KX895005	KX895337	KX895223
	NB2	<i>Podocarpus macrophyllus</i>	China	MW142347	MW147682	MW147689
	NB4	<i>Podocarpus macrophyllus</i>	China	MW142348	MW147683	MW147690
	NB7	<i>Podocarpus macrophyllus</i>	China	MW142349	MW147684	MW147691
	NB11	<i>Podocarpus macrophyllus</i>	China	MW142350	MW147685	MW147692
	NB2-1	<i>Podocarpus macrophyllus</i>	China	MW142351	MW147686	MW147693
	NB3-3 = CFCC 55,875	<i>Podocarpus macrophyllus</i>	China	MW142352	MW147687	MW147694
	NB3-5	<i>Podocarpus macrophyllus</i>	China	MW142353	MW147688	MW147695
<i>P. malayana</i>	CBS 102,220*	<i>Macaranga triloba</i>	Malaysia	KM199306	KM199411	KM199482
<i>P. menhaiensis</i>	CGMCC 3.18250*	<i>Camellia sinensis</i>	China	KU252272	KU252488	KU252401
<i>P. monochaeta</i>	CBS 144.97*	<i>Quercus robur</i>	Netherlands	KM199327	KM199386	KM199479
<i>P. novae-hollandiae</i>	CBS 130,973*	<i>Banksia grandis</i>	Australia	KM199337	KM199425	KM199511
<i>P. oryzae</i>	CBS 353.69*	<i>Oryza sativa</i>	Denmark	KM199299	KM199398	KM199496
<i>P. pallidotheae</i>	MAFF 240,993*	<i>Pieris japonica</i>	Japan	NR111022	LC311584	LC311585
<i>P. pandanicola</i>	MFLUCC 16–0255*	<i>Pandanus</i> sp.	Thailand	MH388361	MH412723	MH388396
<i>P. papuana</i>	CBS 331.96*	Coastal soil	Papua New Guinea	KM199321	KM199413	KM199491
<i>P. parva</i>	CBS 265.37*	<i>Delonix regia</i>	—	KM199312	KM199404	KM199508
<i>P. photinicola</i>	GZCC 16–0028*	<i>Photinia serrulata</i>	China	KY092404	KY047663	KY047662
<i>P. portugalica</i>	CBS 393.48*	—	Portugal	KM199335	KM199422	KM199510
<i>P. rhizophorae</i>	MFLUCC 17–0416*	<i>Rhizophora apiculata</i>	Thailand	MK764283	MK764349	MK764327
<i>P. rhododendri</i>	OP086*	<i>Rhododendron sinogrande</i>	China	KC537804	KC537818	KC537811
<i>P. rhodomyrtus</i>	HGUP4230*	<i>Rhodomyrtus tomentosa</i>	China	KF412648	KF412642	KF412645
<i>P. rosea</i>	MFLUCC 12–0258*	<i>Pinus</i> sp.	China	JX399005	JX399036	JX399069
<i>P. scoparia</i>	CBS 176.25*	<i>Chamaecyparis</i> sp.	—	KM199330	KM199393	KM199478

Table 1 (continued)

Species	Culture accession number ^a	Host/Substrate	Location	GenBank accession number ^b		
				ITS	TUB	TEF
<i>P. sequoiae</i>	MFLUCC 13–0399*	<i>Sequoia sempervirens</i>	Italy	KX572339	—	—
<i>P. shorea</i>	MFLUCC 12–0314*	Dead wing of seed of <i>Shorea obtuse</i>	Thailand	KJ503811	KJ503814	KJ503817
<i>P. sichuanensis</i>	CGMCC 3.18244*	<i>Camellia sinensis</i> 'Mingshan131'	China	KX146689	KX146807	KX146748
<i>Pestalotiopsis</i> sp.	CBS 264.33	<i>Cocos</i> sp.	Indonesia	KM199322	KM199412	KM199490
<i>Pestalotiopsis</i> sp.	LC3616	<i>Camellia</i> sp.	China	KX894990	KX895321	KX895207
<i>Pestalotiopsis</i> sp.	LC6576	<i>Camellia sinensis</i>	China	KX895021	KX895354	KX895240
<i>Pestalotiopsis</i> sp.	CBS 111,576	<i>Leucospermum cunei</i>	USA	MH553961	MH554620	MH554379
<i>Pestalotiopsis</i> sp.	CBS 114,489	<i>Leucospermum</i> 'Pink Ice'	USA	MH553978	MH554637	MH554396
<i>Pestalotiopsis</i> sp.	CBS 143,892	<i>Eucalyptus deglipta</i>	Malaysia	MH554129	MH554802	MH554564
<i>Pestalotiopsis</i> sp.	CBS 143,905	<i>Podocarpus</i> sp.	Australia	MH554153	MH554826	MH554588
<i>Pestalotiopsis</i> sp.	CBS 143,900	<i>Corymbia calophylla</i>	Australia	MH554142	MH554815	MH554577
<i>Pestalotiopsis</i> sp.	CPC 27,641	<i>Banksia attenuata</i>	Australia	MH554145	MH554818	MH554580
<i>Pestalotiopsis</i> sp.	CBS 143,902	<i>Isopogon</i> sp.	Australia	MH554146	MH554819	MH554581
<i>Pestalotiopsis</i> sp.	CPC 27,696	<i>Eucalyptus platytypus</i>	Australia	MH554147	MH554820	MH554582
<i>Pestalotiopsis</i> sp.	CPC 29,456	<i>Banksia</i> sp.	Australia	MH554167	MH554840	MH554602
<i>Pestalotiopsis</i> sp.	GZ1D5	<i>Camellia sinensis</i>	China	KX146681	KX146799	KX146740
<i>P. spathulata</i>	CBS 356.86*	<i>Gevuina avellana</i>	Chile	KM199338	KM199423	KM199513
<i>P. telopeae</i>	CBS 114,161*	<i>Telopea</i> sp.	Australia	KM199296	KM199403	KM199500
<i>P. terricola</i>	CBS 141.69*	Pacific Islands soil	Tahiti	MH554004	MH554680	MH554438
<i>P. thailandica</i>	MFLUCC 17–1616*	<i>Rhizophora apiculata</i>	Thailand	MK764286	MK764352	MK764330
<i>P. trachicarpicola</i>	OP068*	<i>Trachycarpus fortunei</i>	China	JQ845947	JQ845945	JQ845946
<i>P. unicolor</i>	MFLUCC 12–0276*	<i>Rhododendron</i> sp.	China	JX398999	JX399030	—
<i>P. verruculosa</i>	MFLUCC 12–0274*	<i>Rhododendron</i> sp.	China	JX398996	—	JX399061
<i>P. yanglingensis</i>	LC4553*	<i>Camellia sinensis</i>	China	KX895012	KX895345	KX895231
<i>P. yunnanensis</i>	HMAS 96,359*	<i>Podocarpus macrophyllus</i>	China	AY373375	—	—

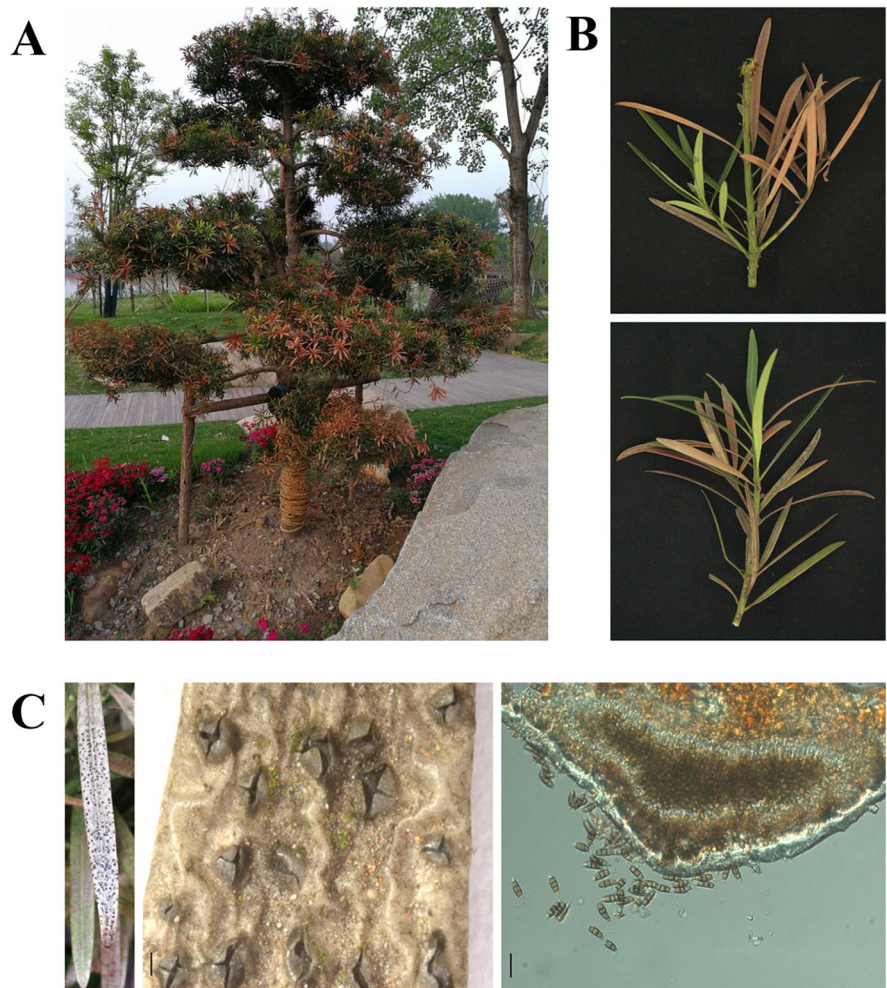
^a CBS: Culture collection of the Centraalbureau voor Schimmelfcultures, Fungal Biodiversity Centre, Utrecht, The Netherlands; CFCC: China Forestry Culture Collection Centre, Institute of Forest Ecological Environment Protection, Chinese Academy of Forestry Sciences, Beijing, China; CGMCC: China General Microbiological Culture Collection Center, Institute of Microbiology, Chinese Academy of Sciences, Beijing, China; ICMP: International Collection of Microorganisms from Plants, Auckland, New Zealand; IFRDCC: International Fungal Research & Development Centre Culture Collection, China; MFLUCC: Mae Fah Luang University Culture Collection, Chiang Rai, Thailand. * = ex-holotype or ex-epitype culture

^b ITS: internal transcribed spacers and intervening 5.8S nrDNA; TUB: partial beta-tubulin gene; TEF: partial translation elongation factor 1-alpha gene

Prior to inoculation, Buddhist pine leaves were surface-sterilized with alcohol (75%), rinsed in sterile water, and air-dried. One wound was made in the middle of the Buddhist pine leaves by a red-hot needle (insect pin, 0.56 mm in diameter). Subsequently, a

mycelial disk (5 mm in diameter) taken from a 4-day-old culture or a 10 µl drop of conidial suspension was placed on each wound. Leaves inoculated with PDA plugs without mycelium or sterile water were employed as controls. The inoculated seedlings were

Fig. 1 Symptoms of leaf blight disease on Buddhist pine. **A** Diseased plant in the field. **B** Diseased shoots of Buddhist pine. **C** Acervuli on dead tissues, including a transverse section view. Bar = 200 μ m for the middle image, and bar = 20 μ m for the right image



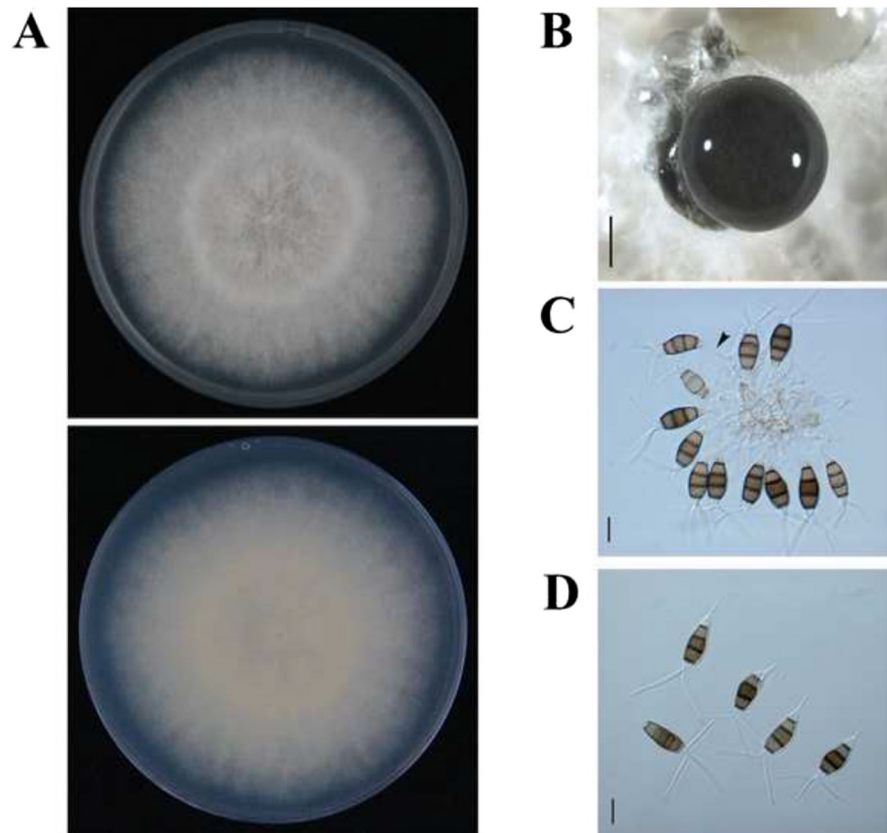
then placed in a climate chamber at 25 °C with high relative humidity (>90%) under a 12 h photoperiod. Ten leaves per isolate were tested for each treatment (one leaf was randomly selected on each plant). The experiment was repeated twice. The lesion length in each treatment was determined after 20 days of inoculation. Statistical analysis was conducted by one-way variance (ANOVA) and means were compared by using Tukey's honest significant difference test ($P=0.05$) in IBM SPSS Statistics software (V22.0, SPSS Inc., Chicago, IL, USA). The pathogen was re-isolated from the inoculated symptomatic leaves, and its identity was confirmed through morphological and molecular tools, as previously described, to fulfil Koch's postulates.

In March 2019, foliar blight was commonly observed on Buddhist pine at Nanping Mountain

Forest Park (Fig. 1). The symptoms of the disease included dark brown lesions on the upper part of leaves at an early stage that later turned grey or brown, with numerous black acervuli scattered on dead tissues (Fig. 1C), and the whole branch was withered in severe cases (Fig. 1).

All seven single-spore isolates collected from symptomatic samples exhibited similar morphologies. The colonies were white during early growth and turned a pale honey colour later. Noticeably, the hyphae were flocculent-like with concentric aerial rings in each colony (Fig. 2A). After 2–3 weeks, black fruiting bodies (conidiomata) were present (Fig. 2B). The conidiophores were subcylindrical, hyaline, unbranched and often reduced to conidiogenous cells (Fig. 2C). The conidiogenous cells were hyaline, clavate or subcylindrical, and ampulliform. The conidia were single,

Fig. 2 Colony morphology and conidial development of *P. lushanensis*. A, Top and reverse view of a colony. B, Conidiomata generated on PDA 20 days after incubation. Bar = 500 μm . C, Conidiophore (indicated by an arrow) and conidiogenous cells. Bar = 10 μm . D, Conidia. Bar = 10 μm



fusoid, medium to deep brown, 4-septate, straight to slightly curved, and $19.2\text{--}28.2 \times 7.1\text{--}9.5 \mu\text{m}$ (av. \pm SD = $22.9 \pm 1.7 \times 7.8 \pm 0.6 \mu\text{m}$); the basal cell was conic, verruculose, hyaline, and $2.5\text{--}5.8 \mu\text{m}$ long; the three median cells were cylindrical or doliiform, $12.7\text{--}17.1 \mu\text{m}$ (av. \pm SD = $14.6 \pm 1.0 \mu\text{m}$) long, and pale brown to brown; the apical cell was conic, hyaline, and $2.8\text{--}4.8 \mu\text{m}$ long, with 2–3 tubular apical appendages (mostly 3), unbranched, $13.7\text{--}28.4 \mu\text{m}$ (av. \pm SD = $19.3 \pm 3.1 \mu\text{m}$) long; and the basal appendage was centric, unbranched, and $3.5\text{--}9.5 \mu\text{m}$ long (Fig. 2D). These features matched those in previous descriptions of the *Pestalotiopsis* genus (Liu et al., 2017).

The sequences of the seven isolates and the reference sequences downloaded from GenBank are listed in Table 1. The analysis of the combined dataset (ITS+TEF+TUB) of our isolates compared to sequences of 74 *Pestalotiopsis* species allowed us to allocate these isolates to molecular groups of known *Pestalotiopsis* species. The alignment of the three-locus concatenated dataset (ITS+TUB+TEF) consisted of

1445 characters (nucleotides and gaps), with 797 constant sites, 439 parsimony-informative sites and 209 parsimony-uninformative sites. The best-fit model of nucleotide substitution in each dataset was deduced according to AICc (HKY+G+I for ITS, K2+G+I for TEF, and HKY+G+I for TUB and the concatenated dataset).

The multigene phylogeny revealed that the seven isolates in this study, including the type specimen LC4344, clustered as a strongly supported monophyletic group (94 bootstrap value; 0.999 posterior probabilities) and were clearly distinguished from the other *Pestalotiopsis* species (Fig. 3). Based on the molecular analysis and morphological characteristics, the seven isolates in this study were identified as *Pestalotiopsis lushanensis* F. Liu & L. Cai (Liu et al., 2017). *P. lushanensis* isolate NB3-3 has been deposited in China Forestry Culture Collection Centre (CFCC 55,875).

The results of the pathogenicity tests showed that all seven *P. lushanensis* isolates were pathogenic on the leaves of Buddhist pine seedlings, regardless of whether mycelial disks or conidial suspensions were used as inocula (Fig. 4), and the symptoms induced

Fig. 3 Phylogenetic tree constructed from the concatenated sequences of the ITS, TUB and TEF regions/genes using the maximum likelihood (ML) and Bayesian inference (BI) method. Thickened branches indicate branches also present in the Bayesian tree with > 0.99 posterior probabilities. The ML bootstrap support values ($> 70\%$) are displayed at the nodes. Ex-type or other authoritative specimens are indicated in bold. *Neopestalotiopsis saprophytica* strain MFLUCC 12–0282 was used as an outgroup

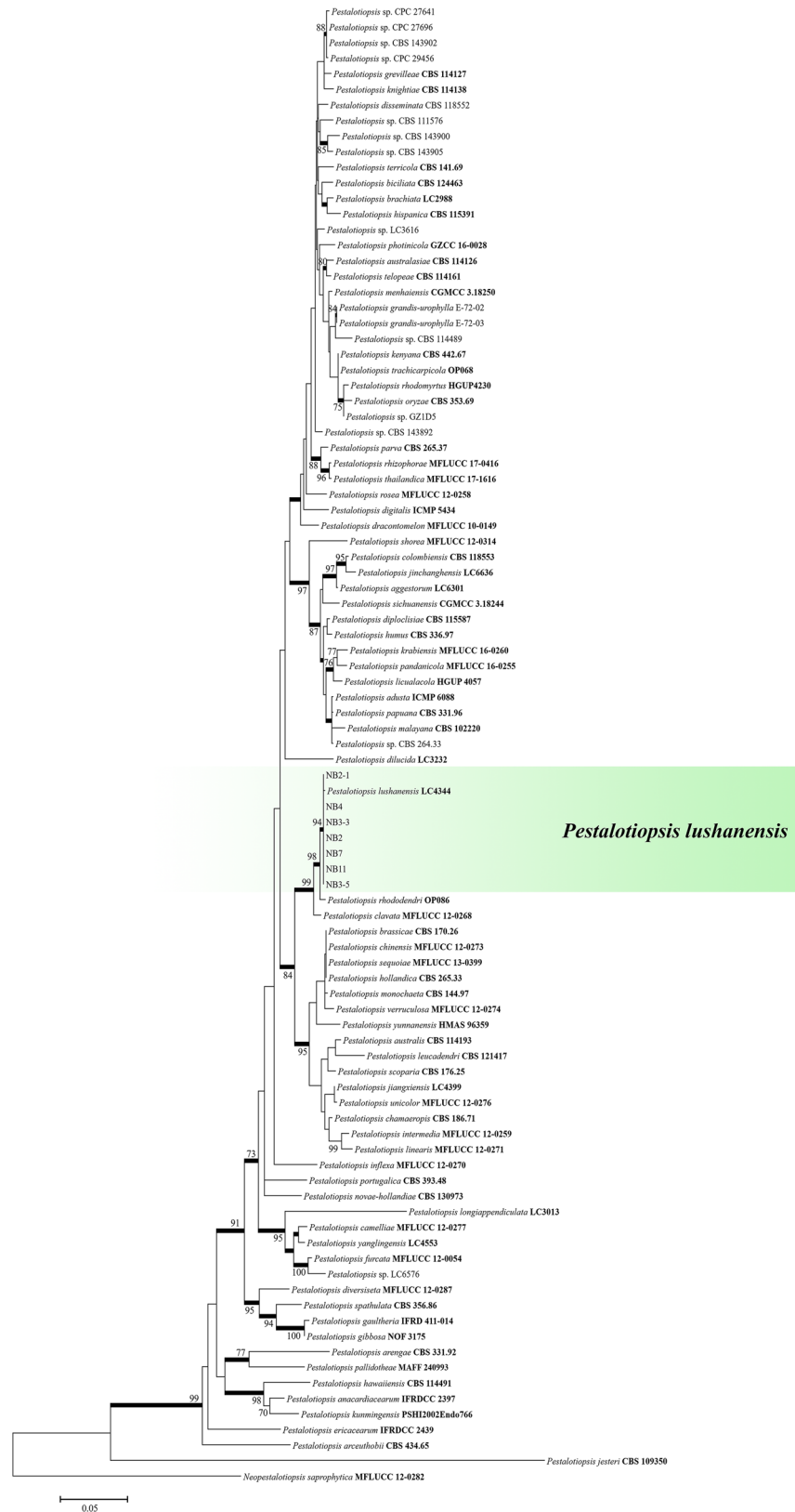
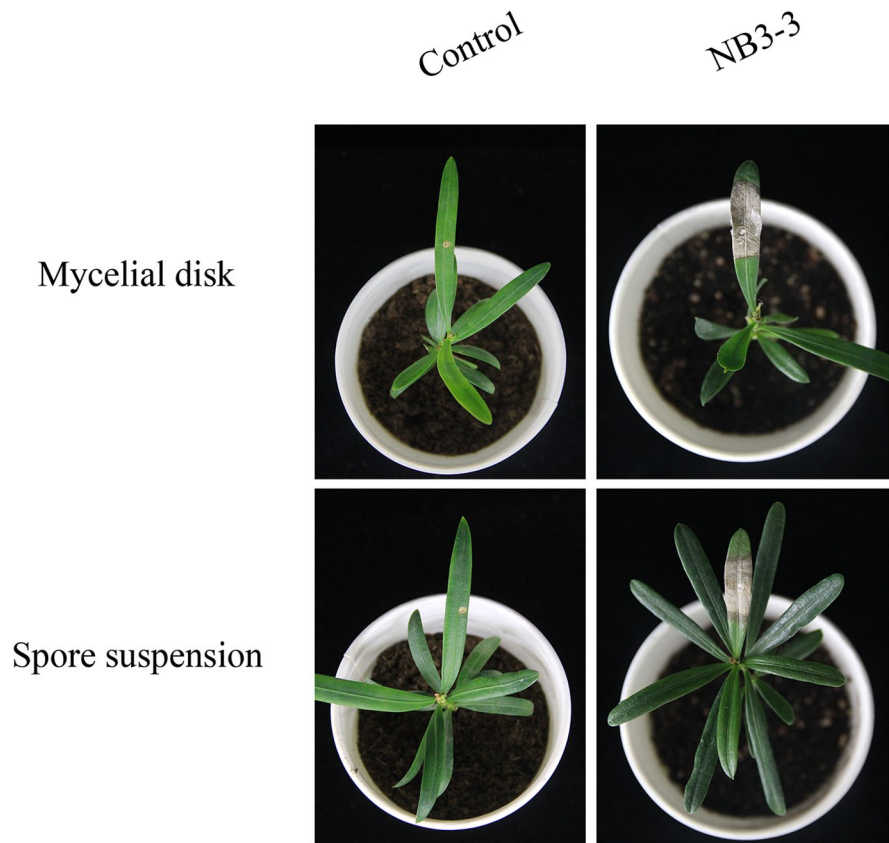


Fig. 4 Pathogenicity test of *P. lushanensis* using a mycelial disk or conidial suspension as the inoculum



were identical to those that occurred in the field. The disease symptoms began as tiny spots around the inoculated site after three days, and then, these spots enlarged to form extensive areas of necrosis 10 days after inoculation, changing in colour from dark brown to taupe. Finally, black acervuli developed on the surface of these lesions. Although all *P. lushanensis* isolates were pathogenic to Buddhist pine leaves,

they showed some differences in virulence. Isolate NB3-3 exhibited the highest virulence, producing typical lesions 10.0 ± 1.8 mm in length when using mycelial disks as inocula and 8.2 ± 1.9 mm in length when using conidial suspensions as inocula (Table 2). The control seedlings inoculated with sterile water or noncolonized PDA disks remained asymptomatic throughout the experiment (Fig. 4). The fungi were

Table 2 Pathogenicity of *P. lushanensis* isolates on Buddhist pine 20 days after inoculation

Species	Isolate	Incidence rate (%) ^a	Lesion diameter (mm) ^a		
			Mycelial disk	Conidial suspension	
<i>P. lushanensis</i>	NB2	90.0 ± 0.0	75.0 ± 5.0	5.6 ± 1.6 cd	4.5 ± 1.8d
	NB4	85.0 ± 5.0	80.0 ± 10.0	7.1 ± 1.9bc	5.4 ± 0.7bc
	NB7	90.0 ± 10.0	80.0 ± 0.0	6.0 ± 1.5 cd	3.9 ± 1.7d
	NB11	85.0 ± 5.0	75.0 ± 15.0	5.5 ± 1.9 cd	4.8 ± 2.0d
	NB2-1	100 ± 0.0	90.0 ± 10.0	7.7 ± 1.9b	6.5 ± 1.6b
	NB3-3	100 ± 0.0	100.0 ± 0.0	10.0 ± 1.8a	8.2 ± 1.9a
	NB3-5	90.0 ± 0.0	65.0 ± 5.0	5.0 ± 1.4d	4.2 ± 1.0d

^a Values were means (± standard deviation [SD]) of two repeated experiments. Means with different letters within columns indicate mean lesion lengths that are significant different (P=0.05)

reisolated from inoculated symptomatic leaves at 100% frequency, and their gene sequences and phenotypic features were identical to those originally determined.

Several *Pestalotiopsis* spp. have been reported to be related to leaf blight disease on Buddhist pine. Among them, *Pestalotiopsis podocarp* isolated from diseased Buddhist pine leaves was determined to be the causal agent in Guizhou Province (Sang et al., 2006), and *Pestalotiopsis virgamla* was reported to cause tip blight disease in Guangxi Province (Su et al., 2015). Based on morphology and virulence tests together with multigene sequence data, this study has verified that *P. lushanensis* is capable of causing leaf blight on Buddhist pine in China and will serve as the basis for further studies towards improved management strategies.

Species in the *Pestalotiopsis* genus have gone largely misidentified when using only phenotypic features or single-gene data, since colony characteristics (e.g., colour, pigment, texture, and growth rate) tend to be variable in *Pestalotiopsis* spp. (Keith et al., 2006). In addition, the DNA sequences of *Pestalotiopsis* species deposited in GenBank might have been incorrectly named in the past (Maharachchikumbura et al., 2011). A previous study pointed out that the ITS region is less informative than the TUB gene for distinguishing species in this genus (Hu et al., 2007). Wang et al. (2019), Shu et al. (2020) and Silva et al. (2020) demonstrated that multilocus phylogenetic analysis (ITS + TUB + TEF) provided better species resolution than using either marker alone. In this study, the phylogenetic tree derived from a combination of ITS, TUB and TEF sequences revealed that all seven isolates were clustered in the *P. lushanensis* clade with a 94 bootstrap support value and 0.999 posterior probabilities.

Regardless of whether a conidial suspension or mycelial disk was used, all seven *P. lushanensis* isolates were pathogenic to wounded Buddhist pine leaves. In contrast, symptoms were not usually induced on non-wounded plants (data not shown), indicating that wounding may be a necessary condition for the development of symptoms. Similar phenomena were observed in previous studies (Chen et al., 2020; Wang et al., 2019). *Pestalotiopsis* spp. may invade plants through wounds with the help of insects, mechanical injury or some unknown factors to induce serious diseases (Bai et al., 2015). Further studies are needed to focus on the origin of the causal agent and disease

cycle. Developing integrated strategies for disease management in the field is also a top priority.

Acknowledgements The author would like to thank the anonymous reviewers for their valuable suggestions on this manuscript.

Funding This study was financially supported by the Postgraduate Research & Practice Innovation Program of Jiangsu Province (KYCX20_0875).

This research article is not submitted elsewhere for publication and complies with the Ethical Rules applicable for this journal.

Declarations

Conflict of interest The authors declare that they have no conflicts of interest.

Animal studies and human participants This article does not contain any studies with human participants or animals performed by any of the authors.

Informed consent All authors consent to this submission.

References

- Akinsanmi, O. A., Nisa, S., Jeff-Ego, O. S., Shivas, R. G., & Drenth, A. (2017). Dry flower disease of *Macadamia* in Australia caused by *Neopestalotiopsis macadamiae* sp. nov. and *Pestalotiopsis macadamiae* sp. nov. *Plant Disease*, 101, 45–53.
- Bai, Q., Zhai, L., Chen, X., Hong, N., Xu, W., & Wang, G. (2015). Biological and molecular characterization of five *Phomopsis* species associated with pear shoot canker in china. *Plant Disease*, 99, 1704–1712.
- Carbone, I., & Kohn, L. M. (1999). A method for designing primer sets for speciation studies in filamentous ascomycetes. *Mycologia*, 91, 553–556.
- Chen, Y., Wan, Y., Zeng, L., Meng, Q., Yuan, L., & Tong, H. (2020). Characterization of *Pestalotiopsis chamaeropsis* causing gray blight disease on tea leaves (*Camellia sinensis*) in Chongqing, China. *Canadian Journal of Plant Pathology*, 43, 413–420.
- Chen, Y., Zeng, L., Shu, N., Jiang, M., Wang, H., Huang, Y., & Tong, H. (2018). *Pestalotiopsis*-like species causing gray blight disease on *Camellia sinensis* in China. *Plant Disease*, 102, 98–106.
- Glass, N. L., & Donaldson, G. C. (1995). Development of primer sets designed for use with the PCR to amplify conserved genes from filamentous ascomycetes. *Applied and Environmental Microbiology*, 61, 1323–1330.
- Hu, H., Jeewon, R., Zhou, D., Zhou, T., & Hyde, K. D. (2007). Phylogenetic diversity of endophytic *Pestalotiopsis* species in *Pinus armandii* and *Ribes* spp.: Evidence from rDNA and beta-tubulin gene phylogenies. *Fungal Diversity*, 24, 1–22.

- Huelsenbeck, J. P., & Rannala, B. (2004). Frequentist properties of Bayesian posterior probabilities of phylogenetic trees under simple and complex substitution models. *Systematic Biology*, *53*, 904–913.
- Jeewon, R., Liew, E., Simpson, J. A., Hodgkiss, I. J., & Hyde, K. D. (2003). Phylogenetic significance of morphological characters in the taxonomy of *Pestalotiopsis* species. *Molecular Phylogenetics and Evolution*, *27*, 372–383.
- Keith, L. M., Velasquez, M. E., & Zee, F. T. (2006). Identification and characterization of *Pestalotiopsis* spp. causing scab disease of Guava, *Psidium guajava*, in Hawaii. *Plant Disease*, *90*, 16–23.
- Kumar, S., Stecher, G., & Tamura, K. (2016). MEGA7: Molecular Evolutionary Genetics Analysis Version 7.0 for Bigger Datasets. *Molecular Phylogenetics and Evolution*, *33*, 1870–1874.
- Liu, F., Bonthond, G., Groenewald, J. Z., Cai, L., & Crous, P. W. (2019). Sporocadaceae, a family of coelomycetous fungi with appendage-bearing conidia. *Studies in Mycology*, *92*, 287–415.
- Liu, F., Hou, L., Raza, M., & Cai, L. (2017). *Pestalotiopsis* and allied genera from *Camellia*, with description of 11 new species from China. *Scientific Reports*, *7*, 866.
- Luo, Y., Zhao, S., Tang, J., Zhu, H., Wei, H., Cui, W., Wang, M., & Guo, P. (2020). White-light emitting diodes' spectrum effect on photosynthesis and nutrient use efficiency in *Podocarpus macrophyllus* seedlings. *Journal of Plant Nutrition*, *43*, 2876–2884.
- Maharachchikumbura, S. S. N., Guo, L., Cai, L., Chukeatirote, E., Wu, W. P., Sun, X., Crous, P. W., Bhat, D. J., McKenzie, E. H. C., Bahkali, A. H., & Hyde, K. D. (2012). A multi-locus backbone tree for *Pestalotiopsis*, with a polyphasic characterization of 14 new species. *Fungal Diversity*, *56*, 95–129.
- Maharachchikumbura, S. S. N., Guo, L., Chukeatirote, E., Bahkali, A. H., & Hyde, K. D. (2011). *Pestalotiopsis*-morphology, phylogeny, biochemistry and diversity. *Fungal Diversity*, *50*, 167–187.
- Maharachchikumbura, S. S. N., Hyde, K. D., Groenewald, J. Z., Xu, J., & Crous, P. W. (2014). *Pestalotiopsis* revisited. *Studies in Mycology*, *79*, 121–186.
- O'Donnell, K., & Cigelnik, E. (1997). Two divergent intragenomic rDNA ITS2 types within a monophyletic lineage of the fungus *Fusarium* are nonorthologous. *Molecular Phylogenetics and Evolution*, *7*, 103–116.
- O'Donnell, K., Kistler, H. C., Cigelnik, E., & Ploetz, R. C. (1998). Multiple evolutionary origins of the fungus causing Panama disease of banana: Concordant evidence from nuclear and mitochondrial gene genealogies. *Proceedings of the National Academy of Sciences of the United States of America*, *95*, 2044–2049.
- Pirone, P. P. (1978). *Diseases and Pests of Ornamental Plants*. Wiley Interscience.
- Ronquist, F., Teslenko, M., Van Der Mark, P., Ayres, D. L., Darling, A., Höhna, S., Larget, B., Liu, L., Suchard, M. A., & Huelsenbeck, J. P. (2012). MrBayes 3.2: Efficient Bayesian phylogenetic inference and model choice across a large model space. *Systematic Biology*, *61*, 539–542.
- Sang, W. Y., Xu, F. L., Yang, R., Ren, C. G., Yang, M. F., & Huang, J. Y. (2006). Investigation on the fungal diseases in the landscape plants in Guiyang. *Forest Pest and Disease*, *6*, 22–25. (In Chinese).
- Shu, J., Yu, Z., Sun, W., Zhao, J., Li, Q., Tang, L., Guo, T., Huang, S., Mo, J., Hsiang, T., & Luo, S. (2020). Identification and characterization of pestalotioid fungi causing leaf spots on mango in southern china. *Plant Disease*, *104*, 1207–1213.
- Silva, A. C., Diogo, E., Henriques, J., Ramos, A. P., Sandoval-Denis, M., Crous, P. W., & Braganca, H. (2020). *Pestalotiopsis pini* sp. nov., an emerging pathogen on stone pine (*Pinus pinea* L.). *Forests*, *11*, 805.
- Su, Y., Zhou, Y., Zhang, Y. M., Wei, J. G., Yun, C. G., & Huang, S. D. (2015). Identification of fungal pathogen of *Podocarpus macrophyllus* leaf disease. *Guangdong Agricultural Science*, *2*, 64–67. (In Chinese).
- Tsai, I., Chung, C. L., Lin, S. R., Hung, T. H., Shen, T. L., Hu, C. Y., Hozzein, W. N., & Ariyawansa, H. A. (2021). Cryptic diversity, molecular systematics, and pathogenicity of genus *Pestalotiopsis* and allied genera causing gray blight disease of tea in Taiwan, with a description of a new *Pseudopestalotiopsis* species. *Plant Disease*, *105*, 425–443.
- Wang, Q., Fan, K., Li, D., Han, C., Qu, Y., Qi, Y., & Wu, X. (2020). Identification, virulence and fungicide sensitivity of *Colletotrichum gloeosporioides* s. s. responsible for walnut anthracnose disease in China. *Plant Disease*, *104*, 1358–1368.
- Wang, S., Mi, X., Wu, Z., Zhang, L., & Wei, C. (2019). Characterization and pathogenicity of *Pestalotiopsis*-like species associated with gray blight disease on *Camellia sinensis* in Anhui Province, China. *Plant Disease*, *103*, 2786–2797.
- Wang, Z., Zhao, Y., & Wei, H. (2017). Chitosan oligosaccharide addition affects current-year shoot of post-transplant Buddhist pine (*Podocarpus macrophyllus*) seedlings under contrasting photoperiods. *iForest*, *10*, 715–721.
- White, T. J., Bruns, T., Lee, S., & Taylor, J. (1990). *Amplification and Direct Sequencing of Fungal Ribosomal RNA Genes for Phylogenetics*. Academic Press.
- Zhang, G. J., Cheng, X. R., Ding, H. X., Liang, S., & Li, Z. (2021). First Report of *Pestalotiopsis lushanensis* Causing Brown Leaf Spot on *Sarcandra glabra* in China. *Plant Disease*, *105*, 424.
- Zheng, X., Zhang, M., Shang, X., Fang, S., & Chen, F. (2020a). First report of *Diaportheeres* causing leaf blight of Buddhist Pine (*Podocarpus macrophyllus*) in China. *Plant Disease*, *104*, 566.
- Zheng, X., Zhang, M., Shang, X., Fang, S., & Chen, F. (2020b). Stem canker on *Cyclocaryapaliurus* is caused by *Botryosphaeria dothidea*. *Plant Disease*, *104*, 1032–1040.